The Astronomical Journal, 125:2521–2530, 2003 May
© 2003. The American Astronomical Society. All rights reserved. Printed in U.S.A.

A DEEP 2MASS SURVEY OF THE LOCKMAN HOLE

C. A. Beichman
Jet Propulsion Laboratory, California Institute of Technology, 4800 Oak Grove Drive, Pasadena, CA 91109;
chas@pop.jpl.nasa.gov

R. Cutri and T. Jarrett
Infrared Processing and Analysis Center, California Institute of Technology, 770 South Wilson Avenue, Pasadena, CA 91125

R. Stiening
Department of Astronomy, University of Massachusetts, 710 North Pleasant Street, Amherst, MA 01003

and

M. Skrutskie
Department of Astronomy, University of Virginia, Charlottesville, VA 22903-0818
Received 2003 January 6; accepted 2003 February 11

ABSTRACT

We have carried out a survey of the Lockman Hole covering over 24 deg^2 using the Two Micron All Sky Survey (2MASS) observing system in a special mode that reaches roughly 1 mag deeper than the nominal 2MASS survey. The resultant point-source catalog reaches to approximately (J, H, K_s) < (17.8, 16.5, 16.0) mag with completeness and reliability in excess of 90%–95% at the faintest levels. These data will be useful in identifying sources in *SIRTF* surveys of this area. We have cataloged 69,115 objects, almost twice as many as in the nominal 2MASS survey of this region. The sample includes a large number of potential new active galaxies, as well as a T dwarf candidate.

Key words: infrared radiation — quasars: general — stars: low-mass, brown dwarfs — surveys

On-line material: machine-readable tables

1. INTRODUCTION

The Lockman Hole (Lockman et al. 1986) is one of the regions of lowest column density of interstellar material in the Milky Way. Accordingly, it has been a target of numerous extragalactic surveys at wavelengths where absorption (X-rays) or emission (infrared) by interstellar gas and dust limit the maximum obtainable sensitivity. Recent surveys of the Lockman Hole include observations by the *Infrared Space Observatory* (Kawara et al. 1998; Elbaz et al. 1999; Fadda et al. 2002), the SCUBA instrument on the James Clerk Maxwell Telescope (Scott et al. 2002), *ROSAT* (Lehmann et al. 2001), *Chandra* (Kenter et al. 2002), and *XMM* (Hassinger et al. 2001). These surveys covered only a relatively small area on the sky, a few tens of square arcminutes up to a square degree. While small areas in the Lockman Hole have been surveyed in the near-IR (Barmby et al. 2002 covered 0.2 deg^2), near-IR data are needed to complement the SWIRE Legacy team's observation of ~10 deg^2 of the Lockman Hole with *SIRTF* (Lonsdale 2001) by providing ancillary information for the reduction and interpretation of *SIRTF* observations.

Although the Two Micron All Sky Survey (2MASS) observed the entire sky in three near-IR wavelengths to sensitivity limits of approximately J, H, and $K_s \sim$ (16.5, 15.5, 15.0) mag or roughly 0.5 mJy (Skrutskie 2001), the enormous sensitivity of *SIRTF*, ~0.007 mJy at 3 μm in the shallow SWIRE survey, puts a premium on sensitive ancillary data obtained over a large area. Cognizant of these needs, we were able to take advantage of observing time available at the end of the 2MASS survey to use the project's 1.3 m telescope located on Mount Hopkins to make a deeper survey of the Lockman Hole region. These observations were interleaved with normal observations but were obtained using a modification of the 2MASS observing strategy (Beichman et al. 1998a; Skrutskie 2001) to integrate 6 times longer than normal (7.8 vs. 1.3 s for each of the six frames that make up a full 2MASS observation). The resultant observations (hereafter denoted "6× data") are approximately 2.5 log $\sqrt{6} = 0.97$ mag deeper than the all-sky survey (hereafter denoted "1×"), reaching 5–7 σ limits of approximately (J, H, K_s) of (17.8, 16.5, 16.0) mag or roughly (0.15, 0.25, 0.25) mJy. Figure 1 shows a side-by-side comparison of the 1× and 6× images of a field containing the red active galaxy candidate discussed later in the text. The increased number of sources in the deeper image is readily apparent.

Images and a source catalog were obtained from these observations using the 2MASS processing pipeline. In this paper we characterize the photometry, astrometry, and completeness and reliability of the 6× results and identify some sources that may prove interesting in upcoming *SIRTF* observations.

Many other regions of sky, totaling over 580 deg^2, were observed in the 6× mode. The uniform processing and release of these data is an important part of the 2MASS Extended Mission that will be carried out over the next 2 years. This paper describes a preliminary reduction of the Lockman Hole data, which is being made available in advance of the launch of *SIRTF*.

2. OBSERVATIONS

2.1. *Region Surveyed*

The Lockman Hole region observed by 2MASS extends from α(J2000.0) = $10^h29^m45^s$ to $11^h00^m33^s$ and from δ(J2000.0) = 54° to 60°. While some 100 μm cirrus is visible

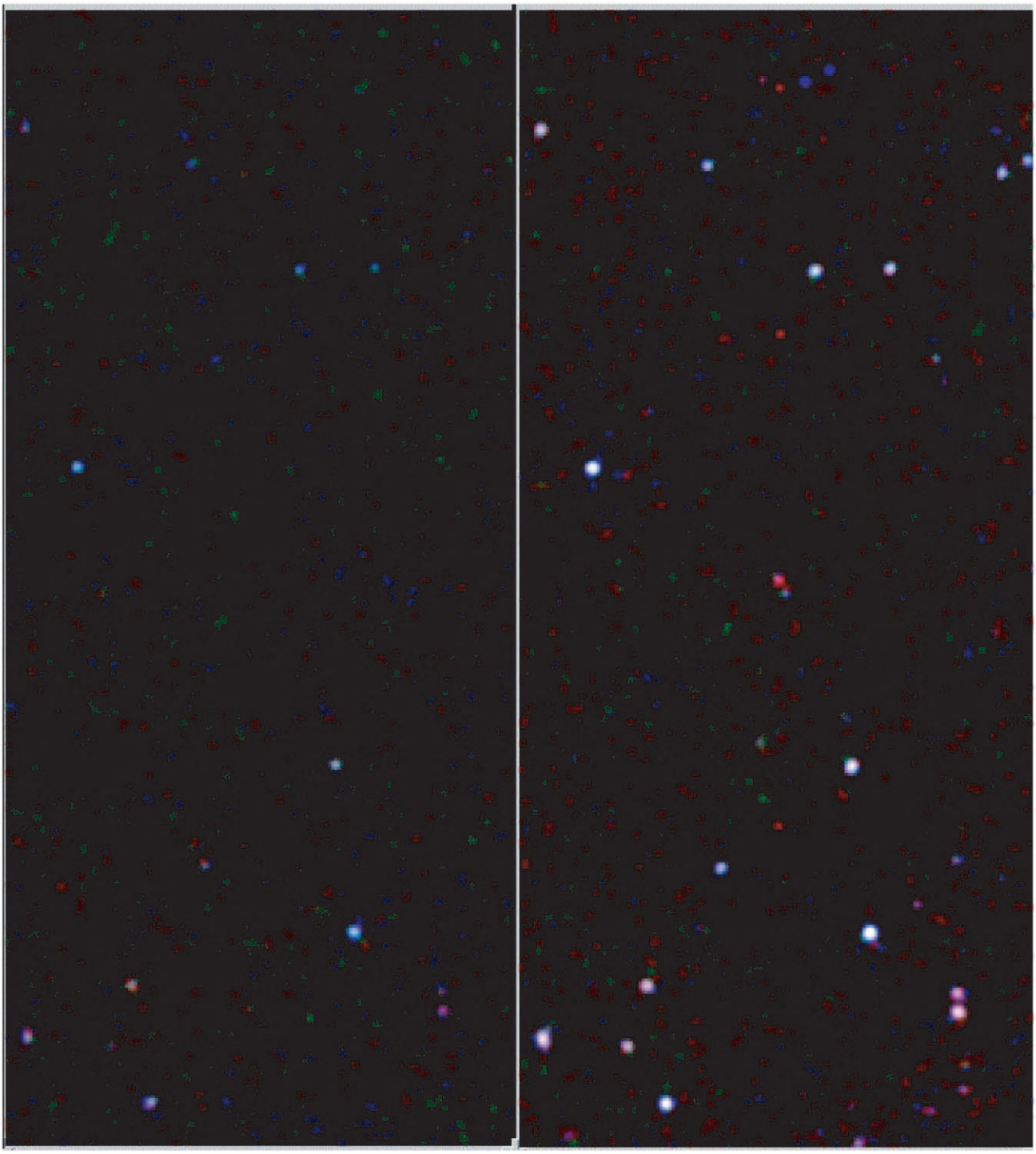

FIG. 1.—Image from the 6 × survey (*right*) shows many more sources than the corresponding area in the 1 × data (*left*). The three 2MASS bands are superposed in this three-color image (*J*: blue, *H*: green, and K_s: red). The very red object at the center of the 6 × image is the candidate active galaxy, 10454723+5729527, described in the text.

in the *IRAS* data, the median cirrus background in this large area is only 0.4 MJy sr^{-1} (Schlegel et al. 1998) making the region well suited to deep surveys at *SIRTF* wavelengths (Fig. 2).

The observing strategy for the 6 × data was identical in all respects to that of the main 2MASS survey, with the exception of the longer integration time. The 2MASS data were obtained using 37 north-going or south-going scans obtained over 14 nights between 2000 March 25 and May 25 (Table 1). The 6° long by 8.′4 wide scans were overlapped by approximately 1′. The quality of the nights was determined using normal 2MASS scans obtained during each night. All nights but one were of excellent quality. The zero point of the photometry on 2000 March 25 is suspect but, as described below, was corrected by reference to 1 × survey scans obtained on other, photometric nights.

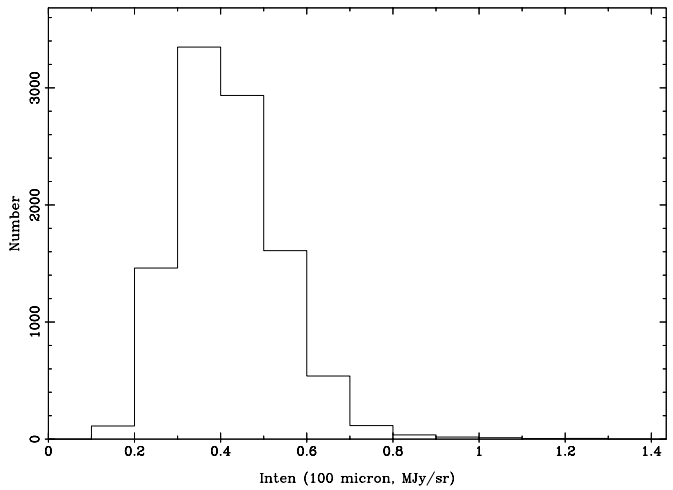

FIG. 2.—Histogram of the 100 μm brightness in the Lockman Hole region surveyed here is based on *IRAS* data (Schlegel et al. 1998) and shows low values of cirrus emission, making the area suitable for deep surveys in the far-IR.

2.2. *Data Reduction*

The *preliminary* processing of the deeper observations reported here required relatively few changes to the 2MASS pipeline (2MASS Explanatory Supplement, Cutri et al. 2002[1]). A scan-by-scan comparison of the 6 × and 1 × observations showed excellent agreement for the ~400 bright stars observed per scan in both data sets: scan-averaged positional agreement within 0.″2 and magnitude agreement within 0.05 mag. A few scans had statistically significant offsets in position (<0.″5) or brightness (<0.09 mag) relative to the 1 × data. Since the 1 × data processing is well characterized, we adjusted the positional and magnitude zero points of each 6 × scan to the mean of the sources in corresponding 1 × scans. As described below, the photometric and astrometric agreement both internal to the 6 × data and relative to the 1 × data is excellent. It is important to emphasize that over the next 2 years of the 2MASS Extended Mission, all the 6 × observations will be reduced with an optimized pipeline, which will result in improved photometry, astrometry, and other characteristics relative to this preliminary reduction.

The extended source portion of the 2MASS pipeline was not run on the 6 × data. Accordingly, the results here pertain only to point sources. Readers interested in extended objects (nearby galaxies) in this region should refer to the standard 2MASS data products.

[1] Available at http://www.ipac.caltech.edu/2mass/releases/second/doc/explsup.html.

2.3. *Overlap Sources*

As a result of the overlap between scans, approximately 15% of all sources were detected twice. To ensure the uniformity of the 1 × 2MASS catalog, the 2MASS catalog generation software selected only one of these sources (based on criteria such as the closeness of the source to the center of the detector array) for inclusion in the final catalog. Since the goal of the 6 × survey is maximum sensitivity, we have taken a different approach. We averaged the positions and magnitudes for all duplicate sources observed on different scans and located within 1.″5 of one another. Sources found within 1.″5 of one another but within the same scan were marked as confused with only the brighter apparition in each band reported.

Simple averages were formed for each band with multiple, valid detections with uncertainties obtained by averaging the individual magnitude uncertainties and dividing by $\sqrt{2}$. The magnitude of a source in the overlap region in a band detected only once was taken to be that of the single valid detection. A band detected in neither apparition was assigned the brightest noise value as an upper limit. An absolute floor on upper limits was set at $(J, H, K_s) = (19.3, 18.0, 17.5)$ mag. In the catalog upper limits that have been modified to reflect these floors are denoted by 8.888 in the magnitude uncertainty columns. As described in the 2MASS Explanatory Supplement, "read flags" denote, on a band-by-band basis, whether a source was detected as a bright source in the short interval of the first read of the array (read flag = 1), as a source of normal brightness on the two reads of the array (read flag = 2), in both modes (read flag = 3), or not at all (read flag = 0). The read flags of sources were combined together to indicate whether a source was observed once or twice in each band, e.g., (read flag = 2) for a single read-2 measurement or (read flag = 4), for two read-2 measurements. Note that these definitions of read flags 3 and 4 differ from those for the main 2MASS catalog.

Positions of sources in the overlap regions were obtained by averaging the two measurements. Positional uncertainties were obtained by averaging the projections of the error ellipses of the two measurements onto the (α, δ) axes, dividing by $\sqrt{2}$, and recombining the result as an error ellipse.

2.4. *Artifacts*

The 2MASS pipeline eliminates a wide variety of false sources due to artifacts of bright sources, including filter glints, diffraction spikes, and persistence echoes. In addition

TABLE 1
LOCKMAN 6 × SURVEY LOG

Date (UT)	Scan	Date (UT)	Scan
2000 Mar 25[a]	34, 35	2000 May 14	14, 15, 23
2000 Apr 29	14, 15, 22, 23, 30, 31	2000 May 19	27, 28
2000 May 04	14, 15, 22, 23	2000 May 20	14, 15, 22, 23
2000 May 05	28	2000 May 23	15, 22, 23
2000 May 10	7, 8, 15, 16	2000 May 24	14, 15, 22, 23
2000 May 13	34, 35	2000 May 25	14, 15

[a] Night not of photometric quality at the 0.1 mag level. The 6 × point-source magnitudes were corrected with respect to 1 × catalog and calibrated images were not produced.

to rejecting sources flagged with any of these artifacts, we made a number of tests to verify that the same software was working effectively on the 6 × data. A powerful test for repeatable artifacts is to search for all objects within ∼90″ of a bright source, (J, H, K_s) < 10 mag, and then to look for groupings of sources above the nominal background source density. This technique was used to develop and tune the basic artifact removal software used in the 1 × pipeline. Application of this technique to the 6 × data using bright sources from the 1 × catalog showed a small enhancement in faint sources located within $\Delta\alpha < \pm 40''$ and $\Delta\delta < \pm 1''$ of the east-west diffraction spikes. These were excised from the source lists, as were a few very faint persistence sources. Examination of the spatial distribution of sources with various combinations of bands revealed a problem with the data from the H-array that led to a large number of faint ($H \sim 16$ mag), spurious, H-only detections in ∼20″ wide stripes up to a few degrees in length, scattered randomly throughout the survey area. Approximately 1200 false, H-only sources were removed by examination of source extractions binned in right ascension.

Sources suspected of being blends of two or more objects were often deblended poorly in the preliminary version of the pipeline. To account for this problem without rejecting a real astrophysical object that was detected properly at other wavelengths, the magnitude of the questionable band was replaced with an upper limit. The upper limit was taken to be the brightest of the magnitudes (or limits) measured in all three wavelengths. These sources have the appropriate magnitude uncertainty set to 8.888 and the confusion flag (cc_flag) set to B.

2.5. *Source Selection*

The emphasis of this paper is finding faint sources that might be counterparts to objects found in high galactic latitude surveys, e.g., the SWIRE Legacy project. Accordingly, our emphasis is on delving as deeply and completely into the data as possible, without compromising the reliability or photometric accuracy of the extracted sources. The 1 × 2MASS catalog limit is based on a source having at least one band with a signal-to-noise ratio (S/N) = 7 detection, based on both local and scan-averaged noise levels. We adopted a selection limit based on the completeness and reliability of the 1 × data, but shifted to reflect the greater sensitivity of the 6 × observations. Analysis of 60 individual 1 × scans (2MASS Explanatory Supplement, Cutri et al. 2002, § VI.4) showed that the differential completeness and reliability were better than 0.90 (and usually better than 0.95) at $16.3 < J < 16.8$ mag, $15.1 < H < 15.6$ mag, and $14.8 < K_s < 15.3$ mag. Since the 6 × data are 0.97 mag more sensitive than the 1 × data, the 6 × completeness and reliability values of the faintest sources should be better than 0.90 ∼ 0.95 at (J, H, K_s) = (17.8, 16.5, 16.0) mag.

All sources in the 6 × catalog satisfy two basic criteria: (1) they have at least one band with a valid detection brighter than (J, H, K_s) = (17.8, 16.5, 16.0) mag; and *either* (2a) one band with a S/N > 7 detection *or* (2b) two bands with S/N > 4 detections. The estimate of SNR is based on fitting the point-spread function to the stellar profile, which results in a magnitude uncertainty given by $\sigma_{\rm mag} = 1.086/({\rm S/N})$ mag. These thresholds are similar to the "local" and "scan" S/N criteria used to generate the 1 × catalog. To further enhance the reliability of the data, bright (S/N > 20) sources seen on only a small fraction (<0.4) of the six possible sightings per band (up to 3 × 6 = 18 sightings for a three-band source) were rejected, as were sources with a poor goodness-of-fit parameter $\chi^2 > 10$ in all detected bands. These criteria are similar to those adopted for the main 2MASS catalog and resulted in the rejection of ∼1000 artifacts due to cosmic rays and meteor trails and, on occasion, double stars and extended sources.

The 6 × data and processing were optimized for improved performance on faint sources, not for accurate photometry of bright stars. The 1 × catalog offers excellent (∼3%) photometry of sources as bright as $J \sim 7$ mag. Thus, to avoid confusion regarding the appropriate data for bright sources seen in both catalogs, stars with any band brighter than J, or H, or $K_s < 10$ mag were excluded from the 6 × catalog; the user should refer to the 2MASS catalog for information on the 533 brightest sources in this region. For the convenience of the user of these data, a file containing the 1 × data for these bright sources is available on-line in a format identical to that used for the 6 × data (Table 5).

3. THE FINAL 6 × CATALOG

The 6 × catalog contains 69,115 sources, almost twice as many as in the 1 × catalog of the same area. Table 2 gives the breakdown of sources in the 6 × catalog for different combinations of wavelength bands along with a comparison of the number of sources seen in the 1 × catalog. On a band-by-band basis the largest difference is the increased fraction of single-band sources at J and K_s in the 6 × catalog. This reflects the relatively faint magnitude limit imposed to optimize for completeness. Of the 69,115 sources in the 6 × catalog, approximately 58% (40,212) have optical counterparts within 1.″5 in the USNO-A catalog (Monet et al. 1998). The fraction of 6 × sources with optical counterparts is consistent with the majority of JHK_s, JH, and J sources being normal stars of progressively fainter magnitude.

The format of the point-source data is described in the Appendix (Table 5), and a sample of the table is given in

TABLE 2
BAND COMBINATIONS IN THE 6 × CATALOG[a]

Band Comb.	6 ×	6 × + USNO	1 ×	Band Comb.	6 ×	6 × + USNO	1 ×
JHK_s	55,198	35,819	32,763	$-HK_s$	399	195	112
$JH-$	5482	2351	2116	$-H-$	52	6	130
$J-K_s$	2068	851	806	$-K_s$	2684	99	257
$J-$	3232	891	1083	Total	69,115	40,212	37,267

[a] J, H, $K_s > 10$ mag in both 1 × and 6 × data sets.

Table 6.[2] This same location can be used to download individual images. Images for the two easternmost scans of the Lockman Hole region are not available because of the nonphotometric quality of that night (2000 March 25).

3.1. *Astrometry*

The astrometric quality of the 6 × data is excellent. The 2MASS-Tycho-2 comparison shows an absolute astrometric dispersion for bright sources of 0.″17 in right ascension and 0.″15 in declination (Fig. 3). This value forms one portion of the astrometric uncertainty quoted in the 6 × catalog. The other component comes from the uncertainties in the PSF-fitting to each individual source. Because the astrometric routines used in the preliminary version of the 6 × pipeline were not fully optimized, the 6 × catalog gives only a single value for the positional uncertainty: the root mean square of the absolute uncertainty relative to the Tycho/*Hipparcos* astrometric reference frame (Perryman et al. 1997), $\sigma_{\rm TYCHO} = (0.15 \times 0.17)^{1/2} = 0.16''$ combined with the harmonic mean of the semimajor (a) and semiminor (b) axes of the error ellipse for the individual source, i.e., $\sigma_{6\times} = (a \times b + \sigma^2_{\rm TYCHO})^{1/2}$. The statistics of sources seen in the overlap regions show a dispersion of $\sigma_{\alpha,\delta}/\sqrt{2} < 0.2''$ for objects with $J < 15$ mag, growing to $\sigma_{\alpha,\delta} \sim 0.''4$ for sources at the catalog limit. Positions of sources in the overlap regions are affected by distortion at the edges of the focal plane, so that the positional accuracy of the typical source will be slightly better than this value (see below).

3.2. *Photometry*

The comparison of the 1 × and 6 × magnitude information reveals excellent agreement between the two data sets at levels below ~10 mag (as described above, the 1 × catalog should be consulted for objects brighter than this level) and for stars as faint the 1 × catalog limit. However, for fainter sources in the 1 × database, the 1 × data show a flux bias relative to the "true" magnitude obtained from the 6 × data (Fig. 4). This well-known "flux overestimation" effect comes about when positive-going noise pushes a faint source above the detection threshold, while negative-going noise makes the source undetectable. The bias reaches ~0.4 mag at the faintest levels. Of course, this flux bias also effects the 6 × data, but at a level 0.97 mag fainter than in the 1 × data. Figure 4 suggests that the flux overestimation bias should be smaller than 0.2 mag in most of the 6 × data.

[2] The point-source file can be obtained from the electronic version of the Astronomical Journal and via ftp from ftp://irsa.ipac.caltech.edu/lockman.html.

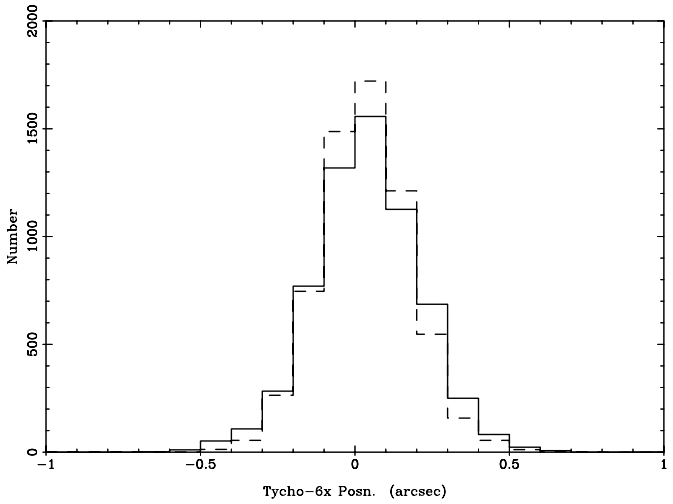

FIG. 3.—Comparison of 6 × positions with optical data for Tycho stars shows a dispersion of 0.″17 in right ascension and 0.″15 in declination.

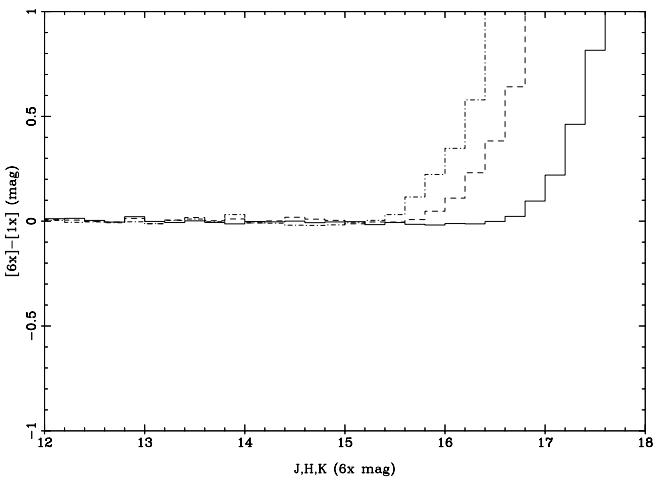

FIG. 4.—Difference between 1 × and 6 × photometry as a function of 6 × brightness shows a flux overestimation (Malmquist bias) for the faintest 1 × sources. J-values are shown as a solid line, H-values as a dashed line, and K_s values as a dash-dot line.

3.3. *Completeness*

We used the 13,000 sources seen twice in overlap regions to assess the completeness of the 6 × data. The completeness is defined as the ratio of the number of observed sightings in a band relative to the total number of possible sightings:

$$\text{Completeness} = \frac{2 \times N_2 + N_1}{2 \times (N_2 + N_1)} ,$$

where N_1 and N_2 are the numbers of sources in the overlap region seen once or twice, respectively, in a given band. Figure 5 shows that the completeness is 0.85 in H and K_s and in excess of 0.95 at J at the nominal magnitude limits of (17.8, 16.5, 16.0) mag, consistent with the scaling from the 1 × catalog mentioned above. Between 11 and 15 mag the average completeness is 0.97–0.98 with a typical dispersion of 0.01 in each 0.25 mag wide bin. At bright levels, the completeness deduced from the overlap regions is reduced from unity by the imperfect alignment of the edges of the arrays, image quality effects at the edge of the focal plane, and the effects of seeing on the detection of multiple stars and galaxies. Analysis of the 1 × catalog indicates that, when adjustments for these edge effects are taken into account, the completeness at bright levels is in excess of 0.99.

With just two coverages it is not possible to assess the reliability of these data, but by extrapolation from the scaled 1 × data we expect that the reliability of the weakest single-band sources will be greater than 0.90 ~ 0.95 and that the reliability of multiband sources will be better than 0.99. However, *it should be recognized that these data are explicitly optimized to identify faint sources, so that a higher degree*

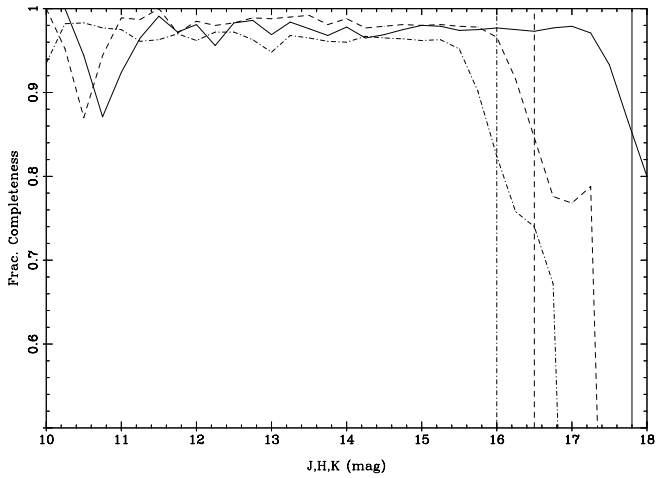

FIG. 5.—Differential 6 × completeness in the three bands derived from sources in the overlap regions between scans. J is shown as a solid line, H as a dashed line, and K_s as a dot-dashed line. The completeness at the survey thresholds is around 85%, as indicated by vertical lines.

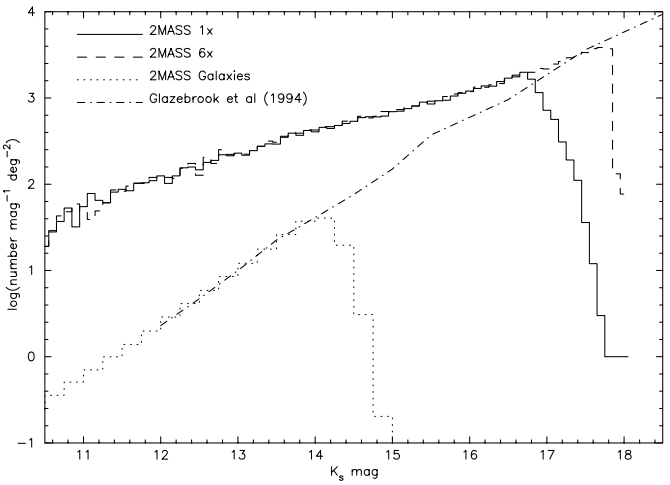

FIG. 7.—Source counts per square degree per magnitude as a function of K_s magnitude in the 1 × and 6 × data set are compared with 2MASS (Jarrett et al. 2000) and deep galaxy counts (Glazebrook et al. 1994).

of unreliability compared with the all-sky 2MASS catalog is to be expected.

3.4. *Comparison with All-Sky Catalog*

A comparison between the 6 × catalog (as corrected in photometry and astrometry with reference to 1 × catalog) the 1 × catalog shows excellent agreement for bright stars with (J, H, K_s) < (14, 13.5, 13) mag. The mean positional offsets were less than 0.″04 with a dispersion $\sigma_{\alpha,\delta}(6\times \text{position} - 1\times \text{position})/\sqrt{2} < 0.''1$. The magnitude offsets between the two data sets were less than 0.01 mag at all wavelengths with a dispersion $\sigma_{J,H,K_s}(6\times \text{magnitude} - 1\times \text{magnitude})/\sqrt{2} < (0.056, 0.065, 0.043)$ mag.

Figure 6 compares integrated source counts between the 6 × and 1 × catalogs. There are approximately twice as many sources in the deeper catalog reaching about a magnitude deeper in all three bands. The small upturn in the source counts (particularly at K_s) just before the completeness drop off is indicative of a few tenths of a magnitude of flux overestimation for the faintest sources. Figure 7 compares the 2MASS source counts with 2MASS galaxies complete to $K_s \sim 13.5$ mag (Jarrett et al. 2000) and deeper K_s galaxy counts (Glazebrook et al. 1994). While stars obviously dominate the brighter magnitudes, galaxies start to dominate the counts at roughly the limit of the 6 × catalog.

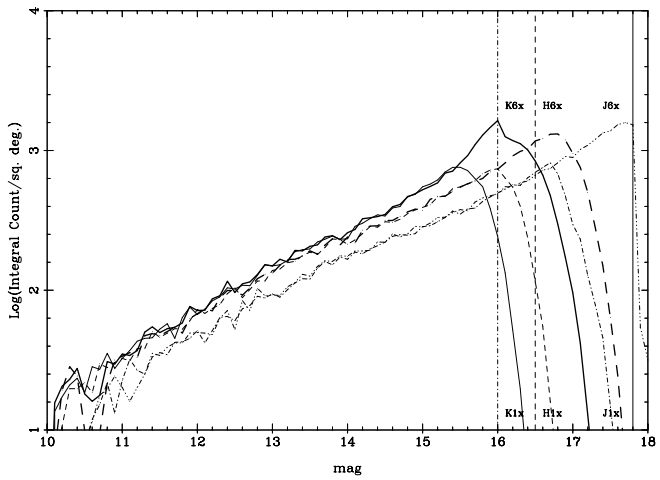

FIG. 6.—Source counts per square degree per magnitude as a function of magnitude in the three bands in the 1 × and 6 × data sets. J is shown as a solid line, H as a dashed line, and K_s as a dot-dashed line. The 6 × curves have the larger values at faint magnitudes. The increase in counts just above the completeness limit at K_s is due to flux overestimation.

4. DISCUSSION

Many objects in the catalog are quite red in $J-K_s$ or $R-K_s$ colors (Fig. 8). While the bulk of these objects are probably late-type stars, some of the most extreme may be identified with red active galaxies (AGNs) and L and T brown dwarfs. It is difficult to identify some of the most interesting objects, because potential optical counterparts of 6 × objects are below the completeness limit of the USNO-A catalog (Monet et al. 1998) used in the 2MASS pipeline. However, even without deeper optical data it is possible to identify a number of interesting sources.

4.1. *AGNs and IR-Bright Galaxies*

Early 2MASS results (Beichman et al. 1998b) hinted at the existence of a new class of AGNs prominent in the near-IR in numbers comparable to or greater than visible and UV-selected AGNs and quasars. Subsequent analysis of the all-sky survey (Cutri et al. 2001) confirmed the existence of this population and showed the objects to be generally underluminous at X-ray wavelengths with evidence for internal absorption (Wilkes et al. 2002). Cross-correlations of the 2MASS 1 × data with radio and X-ray catalogs have strengthened the arguments for the presence of a reddened AGN population (Lonsdale et al. 2000; Helfand et al. 2001; Lacy et al. 2002).

The red AGNs seen in the 1 × catalog are characterized by $J-K_s > 2.0$ mag and a surface density of 0.6 (deg^2)$^{-1}$ at $K_s < 14.5$ mag. Extrapolating this surface density using a simple model for low redshift, optically selected AGNs, which has been modified to include internal absorption (Beichman et al. 1998b; Hewett et al. 1993) to the 6 × catalog limit of $K_s < 16.0$ mag, we expect to find 150–200 objects in 24.3 deg^2 [6–13 (deg^2)$^{-1}$], depending on the range of

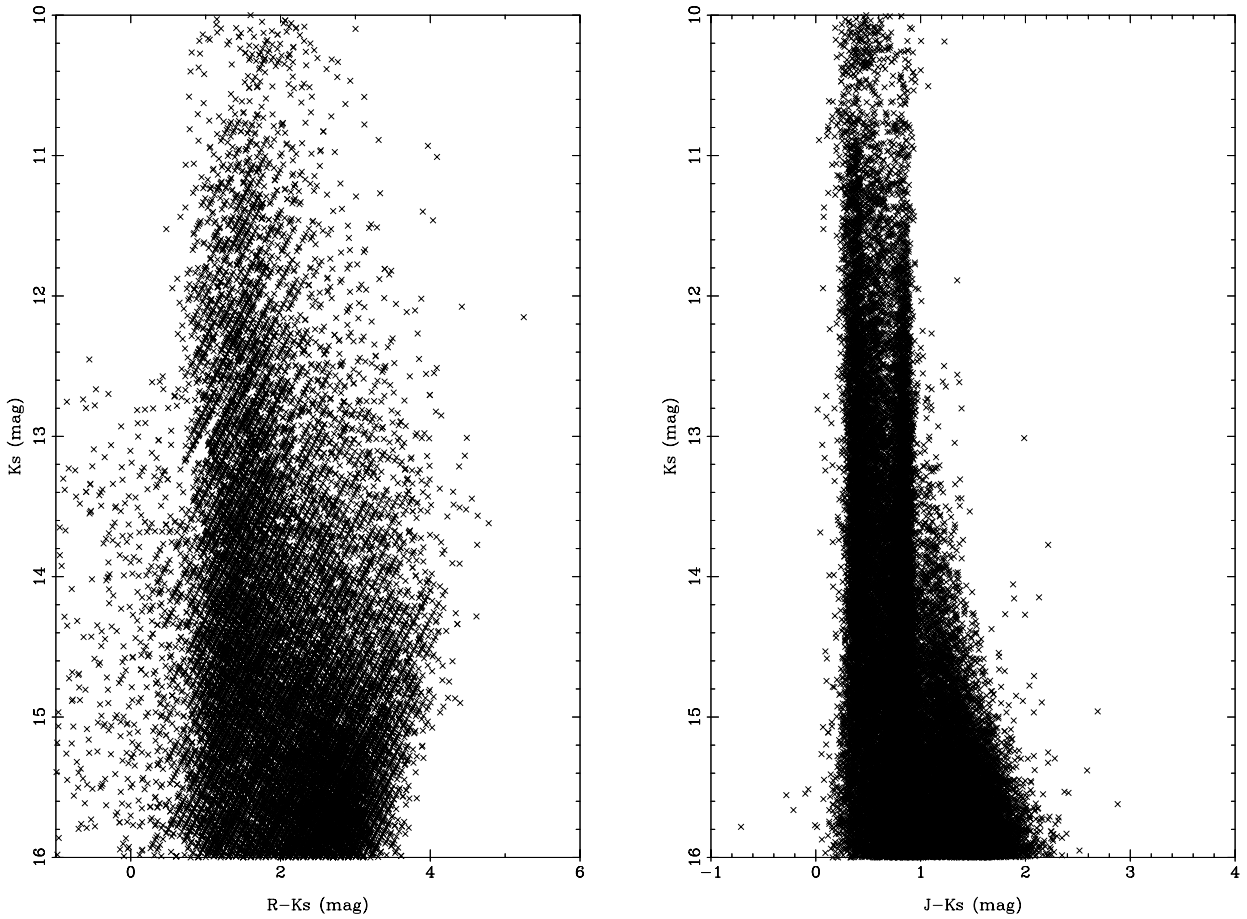

FIG. 8.—As described in the text, color-magnitude plots based on optical and near-IR colors can be used to identify exceptional objects suitable for follow-up observations.

extinction in the overall AGN population. The 6 × catalog contains 176 objects with $J-K_s > 2.0$ mag (Fig. 8, *right*), consistent with this extrapolation. However, spectroscopic follow-up will be required to distinguish between AGNs and galaxies, since fainter galaxies tend to be redder than brighter ones: 2MASS galaxies brighter than $K_s < 13.5$ mag have $J-K_s = 1.25$ mag (Jarrett et al. 2000), while the mean color of a $K = 18$ mag galaxy approaches $J-K_s \sim 2$ mag (Totani et al. 2001).

Table 3 lists some of reddest 6 × sources, i.e., $J-K_s > 2.5$ mag. Of these objects only 10404364+5934090 is previously known; it is an *IRAS* source detected at all four *IRAS* bands. Spectroscopic follow-up shows that it is a Seyfert 1.9 galaxy at a redshift of $z = 0.148$ (Cutri et al. 2001).

The relationship of red 2MASS AGNs to the overall population of active galaxies can be understood by comparison with quasars seen in the Sloan Digital Sky Survey (SDSS; Schneider et al. 2002). Richards et al. (2002) found approximately 18.7 AGNs $(\mathrm{deg}^2)^{-1}$ to a magnitude limit of $i \sim 20.2$ mag. Of these, approximately 13 $(\mathrm{deg}^2)^{-1}$ are low-redshift UV-excess objects, 7.7 $(\mathrm{deg}^2)^{-1}$ are high-redshift objects ($z > 3$), and about 1 $(\mathrm{deg}^2)^{-1}$ are FIRST radio sources (White et al. 1997). Thus, if most of the 6 × 2MASS objects with $J-K_s > 2$ mag turn out to be AGNs, then the 2MASS population *at a brightness limit approximately 2 mag brighter than SDSS limit* represents more than a 50% addition to the low-redshift population found in the SDSS.

TABLE 3
POSSIBLE QUASAR/AGN CANDIDATES

2MASS 6 × (J2000.0)	σ_{pos} (arcsec)	J (mag)	H (mag)	K_s (mag)	B[a] (mag)	R[a] (mag)
10451684+5417137.....	0.55	18.39 ± 0.22	>17.1	15.63 ± 0.24	...	...
10454723+5729527.....	0.30	18.11 ± 0.16	>17.0	15.56 ± 0.07	20.1	19.5
10395163+5804173.....	0.29	17.97 ± 0.15	16.89 ± 0.16	15.38 ± 0.07	...	...
10404364+5934090.....	0.40	14.85 ± 0.02	13.28 ± 0.02	11.84 ± 0.02	18.4	17.5
10502719+5858249.....	0.36	18.50 ± 0.23	17.22 ± 0.19	15.62 ± 0.08	...	...

[a] From USNO-A catalog (Monet et al. 1998).

TABLE 4
POSSIBLE T DWARF CANDIDATES

2MASS 6 × (J2000.0)	σ_{pos} (arcsec)	J (mag)	H (mag)	K_s (mag)	POSS-II[a]
11002592+5512304.....	0.30	16.84 ± 0.06	16.64 ± 0.12	16.44 ± 0.17	Definite faint B, R, I
10450154+5538314.....	0.35	17.14 ± 0.08	16.95 ± 0.18	16.80 ± 0.25	Definite faint B, R, I
10465810+5940592.....	0.30	16.66 ± 0.06	16.43 ± 0.13	16.37 ± 0.17	Definite faint B, R, I
10433964+5958360.....	0.28	16.14 ± 0.04	16.30 ± 0.10	16.12 ± 0.14	No B, possible very faint R (>21 mag), definite faint I (~20 mag)

[a] Estimated from POSS-II images.

We can assess whether SDSS can identify these very red quasars by examining the SDSS color selection criteria for quasars (Richards et al. 2002). For example, if we redden the average QSO spectral energy distribution (Elvis et al. 1994) by the addition of $A_V = 1.5$ mag, then the average $J-K_s$ color (at $z = 0$) increases from 2.0 mag to $J-K_s = 2.3$ mag and the visible colors redden by correspondingly greater amounts. Such objects move from the center of the (*ugriz*) color space of UV-excess AGNs (*blue dots*, Fig. 13 in Richards et al. 2002) to the extreme red end of UV-excess AGN population and into the loci near the FIRST radio sources (*green symbols*, same figure). Note that the 2MASS AGN candidates are not, however, identical with FIRST sources, since only three of the 196 matches between the 2MASS and FIRST catalogs (below the $\delta = 57.^{\circ}5$ limit of the radio survey) have $J-K_s \geq 2$ mag. A detailed comparison of 2MASS and SDSS colors of quasars will lead to specific SDSS criteria tuned to finding such objects in the more sensitive SDSS database. This procedure will lead to a full accounting of AGNs over a wide range of internal reddening, at least up to $A_V < 5$ mag where 2MASS becomes more sensitive to reddened objects than the SDSS (Beichman et al. 1998b).

Finally, we will be able to verify that the red $J-K_s$ color of these objects is due to internal absorption by using *SIRTF* to show that the absorbed radiation emerges at longer wavelengths. By equating the energy absorbed between 0.1 and 10 μm to that emitted by, say, an 80 K blackbody (a representative value for the warm SED seen toward AGNs, Sanders & Mirabel 1996), it is possible to estimate the far-infrared brightness of such a source. For example, 10404364+5934090, with an observed K_s flux density of 12 mJy (Table 3), would be predicted in this simple model to have a 60 μm brightness of 700 mJy. This is comparable to the observed brightness of this object, $F_\nu(60\ \mu\text{m}) = 770$ mJy (*IRAS* Faint Source Catalog, 1990). Similarly, an Elvis-standard AGN reddened by $A_V = 1.5$ mag and detected at the limit of the 6 × catalog (0.25 mJy at 2.2 μm) would emit approximately 20 mJy at 70 μm and be readily detectable in a shallow *SIRTF* survey.

4.2. *Brown Dwarfs*

Estimates of the number of L and T dwarfs come from analysis of the 1 × 2MASS data. From Kirkpatrick et al. (1999) and Reid et al. (1999) there are roughly 0.05 L dwarfs per square degree at $K_s < 14.5$ mag. Assuming an isotropic distribution of objects and a K_s limit of 16.0 mag, there could be $0.05\ (\text{deg}^2)^{-1} \times 24.3\ \text{deg}^2 \times 10^{-0.6 \times (14.5-16\ \text{mag})} \sim 10$ L dwarfs in the 6 × field. Similarly, there should be roughly 8×10^{-4} T dwarfs per square degree at $J < 16$ mag (Burgasser 2002, Table 2.8). Extrapolating to $J < 17.8$ mag, we should find $8 \times 10^{-4}\ (\text{deg}^2)^{-1} \times 24.3\ \text{deg}^2 \times 10^{-0.6 \times (16-17.8\ \text{mag})} \sim 0.24$ T dwarfs. Identification of L dwarfs will require deeper optical data than are presently available, and, using only near-IR colors, it is easy to confuse L dwarfs seen only in 2MASS with more numerous late-M dwarfs. On the other hand, T dwarfs have blue colors in the near-IR because of methane absorption at H and K_s and very red $R-J$ or $I-J$ colors due to the coolness of their atmospheres (<1500 K, Burgasser 2002). We searched the 6 × catalog for objects with $\sigma_{J,H,K_s} < 0.25$ mag, $J-H < 0.25$ mag, $H-K_s < 0.25$ mag, but with no optical counterpart in the USNO-A catalog. Eight objects met these criteria. Inspection of the digitized POSS and the 2MASS images revealed that four of the sources were associated with multiple or bright stars that were missed in the USNO-A catalog; these are not considered further. The remaining four objects (Table 4) have only very faint objects on the POSS-II plates. One object, 10433964+5958360, has no counterpart on the blue POSS-II plate, a very faint counterpart on the red POSS-II plate ($R > 21$ mag, if it exists at all), and a faint counterpart ($I \sim 20$ mag) on the "infrared" POSS-II image. On the basis of its blue near-IR colors, $J-H = -0.16 \pm 0.10$ mag and $H-K_s = 0.18 \pm 0.17$ mag and its $R-J > 5$, $I-J > 4$ mag colors, the object appears to be an early T dwarf (Burgasser 2002). A conclusive identification awaits spectroscopic follow-up.

5. CONCLUSION

In addition to its utility as a deeper catalog for the high Galactic latitude science already enabled by 2MASS, this data set will be particularly useful for observers planning and reducing data from *SIRTF* observations of the Lockman Hole. Releases of a large body of 6 × data covering a few hundred square degrees in many parts of the sky are planned as part of the extended mission for the 2MASS project. These Lockman Hole will be re-reduced using a refined 6 × pipeline, but the existing data set will provide users of *SIRTF* and other facilities with a deeper look at the near-IR sky than previously possible.

This work was performed under contract to Jet Propulsion Laboratory from the National Aeronautics and Space Administration. This publication makes use of data products from the Two Micron All Sky Survey, which is a joint project of the University of Massachusetts and the Infrared Processing and Analysis Center/California Institute of Technology, funded by the NASA and the National Science Foundation. This research has also made use of the NASA/IPAC Extragalactic Database, which is operated by JPL,

Caltech, under contract with NASA. C. A. B. acknowledges useful discussions with Davy Kirkpatrick.

APPENDIX

FORMAT OF THE 6 × POINT-SOURCE CATALOG AND IMAGES

The source information in the 6 × data set is contained in a single ASCII text file following the format given in Table 5. The meaning of most of the columns is as defined for the 1 × catalog in the 2MASS Explanatory Supplement (Cutri et al. 2002). Other columns are discussed in the text or in the notes to the table. A sample of the table is given in Table 6. In addition, the 1 × data for 533 sources with at least one band brighter than 10 mag are included in a table in the format given in Table 5.

The uncompressed image data can be obtained through the image server located at http://irsa.ipac.caltech.edu/lockman.html. Like all 2MASS images, these FITS images have 500 × 1000 1″ pixels with fully descriptive headers. A list of central positions keyed to the file names of the 2427 images in the three bands is also available at that site. Table 7 lists the image filename and central right ascension and declination for each image in J2000.0 decimal degrees. The filename consists of the UT date (YYMMDD), the hemisphere of the observatory (n), the waveband (*j*, *h*, *k*), a three-digit scan number, and a four-digit image number.

TABLE 5
FORMAT OF LOCKMAN HOLE POINT-SOURCE DATA TABLE

Column[a]	Comment
Right ascension (decimal deg)	J2000.0
Declination (decimal deg)	J2000.0
2MASS6 × designation (HMS, DMS)	J2000.0 sexigesimal position in HHMMSSSS, DDMMSSS format[b]
Positional uncertainty (arcsec)	Uncertainty in single position axis
J (mag)	Source magnitude
σJ (mag)	Source magnitude; 9.999 or 8.888 denotes upper limit
H (mag)	Source magnitude
σH (mag)	Source magnitude; 9.999 or 8.888 denotes upper limit
K_s (mag)	Source magnitude
σK_s (mag)	Source magnitude; 9.999 or 8.888 denotes upper limit
Read flag for *J*, *H*, K_s (char)	0 = no detection, 1 = read-1 detection, 2 = read2-read1 detection, 4 = read2–read1 detection on two apparitions
Blend flag for *J*, *H*, K_s (char)	0 = no detection, 1 = one source, 2 = attempt to break up source into two sources (assign upper limit)
Confusion flag for *J*, *H*, K_s	All flags rejected except B for blend.
B mag (mag)	Blue magnitude from USNO-A catalog, 99.99 denotes upper limit
R mag (mag)	Red magnitude from USNO-A catalog, 99.99 denotes upper limit
R opt (arcsec)	Separation between optical source and 2MASS

[a] Most of these columns are the same as defined in the 1 × catalog. The reader is referred to the 2MASS Explanatory Supplement (Cutri et al. 2002) for further information.
[b] For right ascension the SSSS is quoted in centiseconds of time. For declination the SS is quoted in deciseconds of arc.

TABLE 6
SAMPLE OF LOCKMAN HOLE POINT-SOURCE DATA

R.A.[a] (J2000.0)	Decl. (J2000.0)	2MASS Designation	σ_{Pos}	*J* (mag)	σ_J	*H* (mag)	σ_H
157.569620	53.852554	10301670 + 5351091	0.24	17.280	0.063	16.653	0.119
158.296415	53.853027	10331113 + 5351108	0.20	15.363	0.032	14.766	0.038
157.557442	53.853473	10301378 + 5351125	0.22	17.113	0.059	16.327	0.091
160.018018	53.853981	10400432 + 5351143	0.22	16.818	0.065	15.773	0.082
157.717791	53.854700	10305226 + 5351169	0.24	17.698	0.095	16.964	0.137

K_s (mag)	σ_K	Read	Blend	Conf.	*B* (mag)	*R* (mag)	O-IR posn. (arcsec)
16.382	0.126	222	111	000	19.90	18.60	0.05
14.600	0.036	222	111	000	19.70	18.10	1.04
15.780	0.082	222	111	000	19.70	18.50	0.19
15.398	0.084	222	111	000	19.30	18.30	0.51
16.100	0.094	222	111	000	99.99	99.99	0.00

NOTE.—Table 6 is available in its entirety via the link to the machine-readable version above. A portion is shown here for guidance regarding its form and content. The complete version of this table is also available at ftp://irsa.ipac.caltech.edu/lockman.html.
[a] See Table 1 for a description of the columns.

TABLE 7

CENTRAL POSITIONS OF IMAGES IN LOCKMAN HOLE SURVEY

Filename	R.A. (J2000.0) (deg)	Decl. (J2000.0) (deg)
000429n_hi0140009.fits	157.981898	59.867151
000429n_hi0140021.fits	157.982137	59.597707
000429n_hi0140033.fits	157.982372	59.328263

NOTE.—Table 7 is available in its entirety via the link to the machine-readable version above. A portion is shown here for guidance regarding its form and content. The complete version of this table is also available at ftp://irsa.ipac.caltech.edu/lockman.html.

REFERENCES

Barmby, P., Huang, J.-S., Willner, S. P., & Eisenhardt, P. 2002, BAAS, 199, 07.09
Beichman, C. A., Chester, T. J., Cutri, R., Lonsdale, C. J., Kirkpatrick, D., Smith, H. E., & Skrutskie, M. 1998b, PASP, 110, 367
Beichman, C. A., Chester, T. J., Skrutskie, M., Low, F. J., & Gillett, F. 1998a, PASP, 110, 480
Burgasser, A. 2002, Ph.D. thesis, Caltech
Cutri, R. M., Nelson, B. O., Kirkpatrick, J. D., Huchra, J. P., & Smith, P. S. 2001, BAAS, 198, 33.17
Cutri, R. M. et al. 2002, 2MASS Explanatory Supplement
Elbaz, D., et al. 1999, A&A, 351, L37
Elvis, M., et al. 1994, ApJS, 95, 1
Fadda, D., Flores, H., Hasinger, G., Franceschini, A., Altieri, B., Cesarsky, C. J., Elbaz, D., & Ferrando, Ph. 2002, A&A, 383, 838
Glazebrook, K., Peacock, J. A., Collins, C. A., & Miller, L. 1994, MNRAS, 266, 65
Hassinger G., et al. 2001, A&A, 365, L45
Helfand, D. J., Glikman, E., Becker, R. H., White, R. L., Lacy, M., & Gregg, M. D. 2001, BAAS, 198, 33.18
Hewett, P. C., Foltz, C. B., & Chaffee, F. C. 1993, ApJ, 406, L43
Jarrett, T. H., Chester, T., Cutri, R., Schneider, S., Skrutskie, M., & Huchra, J. P. 2000, AJ, 119, 2498
Kawara, K., et al. 1998, A&A, 336, L9
Kenter, A., Murray, S., & Meehan, G. 2002, BAAS, 119, 17.108
Kirkpatrick, D., et al. 1999, ApJ, 519, 802
Lacy, M., Gregg, M. D., Becker, R. H., White, R. L., Glikman, E., & Helfand, D. J. 2002, BAAS, 200, 05.03
Lehmann, I., et al. 2001, A&A, 371, 833
Lockman, F. J., Jahoda, K., & McCammon, D. 1986, ApJ, 302, 432
Lonsdale, C. 2001, BAAS, 198, 25.0
Lonsdale, C. J., Voges, W., Boller, Th., & Wolstencroft, R. D. 2000, BAAS, 197, 90.05
Monet, D. G., et al. 1998, BAAS, 193, 12.003
Perryman, M. A. C., et al. 1997, A&A, 323, L49
Richards, G. T., et al. 2002, AJ, 123, 2945
Reid, I. N. et al. 1999, ApJ, 521, 613
Sanders, D., & Mirabel, I. F. 1996, ARA&A, 34, 749
Schlegel, D., Finkbeiner, D., & Davis, M. 1998, ApJ, 500, 525
Schneider, D. P., et al. 2002, AJ, 123, 567
Scott, S. E., et al. 2002, MNRAS, 331, 817
Skrutskie, M. 2001, BAAS, 198, 33.01
Totani, T., Yoshii, Y., Maihara, T., Iwamuro, F., & Motohara, K. 2001, ApJ, 559, 592
White, R. L., Becker, R. H., Helfand, D. J., & Gregg, M. D. 1997, ApJ, 475, 479
Wilkes, B. J., Schmidt, G. D., Cutri, R. M., Ghosh, H., Hines, D. C., Nelson, B., & Smith, P. S., 2002, ApJ, 564, L65